




A Generalized Storage Function Model for the Water Level Estimation Using Rating Curve Relationship

Saritha Padiyedath Gopalan^{1,2}  · Akira Kawamura¹ · Hideo Amaguchi¹ · Gubash Azhikodan¹

Received: 18 January 2020 / Accepted: 27 May 2020 /
Published online: 6 June 2020
© Springer Nature B.V. 2020

Abstract

This study proposes a novel generalized storage function (GSF) model for water level estimation from the rating curve relationship by considering (i) the spatial distribution of rainfall over the basin and (ii) incorporating all the possible inflow and outflow components to reduce the uncertainties involved. The proposed GSF model, along with three other models, was then applied in two watersheds of Japan to examine its applicability in different types of watersheds with optimized parameters: (i) the Iga watershed, a semi-urban watershed and (ii) the Oto watershed, a rural watershed. Further, the proposed model's effectiveness was identified based on hydrograph reproducibility, Akaike information criterion, and Akaike weight. The results showed that the GSF model performed well in both watersheds compared to the other models. Moreover, the Morris global sensitivity method has used to analyze the sensitivity of the GSF model parameters for the objective function of root mean square error.

Keywords GSF model · Rainfall spatial distribution · SCE-UA global optimization · Akaike information criterion · Morris sensitivity method · Hydrograph reproducibility

Electronic supplementary material The online version of this article (<https://doi.org/10.1007/s11269-020-02585-6>) contains supplementary material, which is available to authorized users.

✉ Saritha Padiyedath Gopalan
charu666@gmail.com

Akira Kawamura
kawamura@tmu.ac.jp

Hideo Amaguchi
amaguchi@tmu.ac.jp

Gubash Azhikodan
gubash@tmu.ac.jp

Extended author information available on the last page of the article

1 Introduction

Floods are considered as severe natural hazards due to the associated flood risk and costs in both rural and urban areas (Karbasi et al. 2018). The flood events will always affect the nearby population. This will indirectly cause an enormous threat to human life, properties, and crops (Seckin and Guven 2012). Flood mitigation is a water management strategy that can control the devastating impact of floods (Bubeck et al. 2012). However, accurate prediction of the hydrograph is necessary for flood mitigation to avoid losses resulting from floodplain inundation. Further, flood peak estimation is also required for the design of bridges, culverts, waterways, etc. (Sahoo and Saritha 2015). For these purposes, rainfall-runoff models are essential tools, and they play a central role in water management.

The simple rainfall-runoff models are lumped and conceptual in their approach to provide information regarding different watershed processes (Andrews et al. 2011). Among them, storage function (SF) models have been widely used in many parts of the world. Kimura (1961) proposed the first SF model (3-parameter) and is still widely used for flood prediction. Subsequently, several improved SF models have been proposed in terms of how to express its nonlinearity, model structure, and the storage hysteresis loop (Hoshi and Yamaoka 1982; Prasad 1967; Sugiyama et al. 1997). However, all these models require effective rainfall as their input for the prediction of direct runoff. This further involves the problems of baseflow separation and effective rainfall estimation. Later, to overcome these problems, Baba et al. (1999) introduced an SF model with loss mechanism (directly uses the observed rainfall and total runoff). Later, Takasaki et al. (2009) developed a new urban SF (USF) model for urban watersheds with the combined sewer system. The performances of different SF models have already evaluated for an urban watershed, and it has found that the USF model performs better in comparison to the conventional SF models (Padiyedath et al. 2018a; Padiyedath et al. 2018b). However, the target area of the USF model is restricted to urban watersheds with the combined sewer system.

Generally, in conventional SF models, a spatially averaged basin rainfall is considered. However, under actual conditions, there is spatial variability in rainfall across a catchment which has not captured when undertaking lumped catchment modelling. This spatial variability will be quite high even in small watersheds based on meteorological factors. Besides, there might be problems with the location of the rain gauges in terms of capturing the representative rainfall corresponding to each rainfall event, particularly for catchments with high rainfall gradients (Vaze et al. 2012). Therefore, the use of basin-average rainfall will further underestimate or overestimate the storm runoff based on meteorological factors as well as the location of rainfall occurrence. Vaze et al. (2011) has investigated the effect of different rainfall data sets on the calibration and simulation of conceptual rainfall-runoff models and concluded that considerable improvement could be obtained in the modelled runoff with better spatial rainfall representation.

All the existing SF models require discharge data for their calibration and subsequent runoff analysis. This observed river discharge is generally obtained from water level observations made at a gauging station which are further converted to flow estimates using a well-defined and stable rating curve (Vaze et al. 2012). However, there are uncertainties in the converted discharge data resulting from errors in the rating curves derived from stream gauging operations as well as a result of extrapolation outside the limits of the rating curve (Sivapragasam and Muttill 2005). This will further contribute to model prediction uncertainties, and several studies have analyzed the uncertainties in discharge estimation from the rating curve (Chen et al. 2013; Domeneghetti et al. 2012; Vatanchi and Maghrebi 2019). In addition, data for a

much larger period is needed to establish a stable rating curve, and it is difficult to update them from time to time.

The direct use of observed water level for model development will be a reliable alternative to reduce the propagation of uncertainty to runoff predictions. In addition, from a disaster perspective, the prediction of water level information is often sufficient to provide an early warning of flooding and to implement evacuation activities. This approach also attempts to reduce the uncertainty derived from the spatial variability of basin rainfall by introducing the rainfall factor, hereafter termed as γ , which will act as a correction coefficient of the basin-average rainfall. Therefore, this study proposes a novel generalized storage function (GSF) model for water level prediction by incorporating the rainfall factor (γ), and all the possible inflow and outflow components. This proposed model could apply in ungauged and partially gauged watersheds, where the rating curve establishment is highly uncertain.

2 Methods

2.1 GSF Model for Water Level Prediction

GSF model considered all the possible inflow and outflow components in a conceptual watershed, as shown in Online Resource 1. The inflow components are represented by rainfall, R (mm/min) and inflows from other basins, I (mm/min). The outflow components comprise the river discharge, Q (mm/min); evapotranspiration, E (mm/min); water intake from the basin, O (mm/min); and groundwater-related loss, q_l (mm/min). The storage equation of GSF model is given as (Hoshi and Yamaoka 1982):

$$s = k_1(Q)^{p_1} + k_2 \frac{d}{dt}(Q)^{p_2} \quad (1)$$

where s is storage (mm); t is time (min); and k_1 , k_2 , p_1 , and p_2 are model parameters. In Eq. (1), Q is replaced with the rating-curve relationship based on power law as follows:

$$Q = a(H-b)^\beta \quad (2)$$

in which a and β are the rating curve constants, and b is a constant that represents the gauge reading corresponding to zero discharge (Domeneghetti et al. 2012). Q is the observed river discharge in m^3/s that was further converted into mm/min in order to use in the continuity Eq. (4) since the other components of Eq. (4) are in mm/min. There value of β in the present study is taken as two based on the assumption of a quadratic rating curve relationship from previous studies for water level and discharge prediction using different models (Takasaki et al. 2005; Tamura et al. 2013). The resulting rating curve relationship is $Q = a(H-b)^2$. The rating curve constants a and b were considered as the GSF model parameters during calibration. Therefore, the storage equation of the GSF model is,

$$s = k_1 \left(a(H-b)^2 \right)^{p_1} + k_2 \frac{d}{dt} \left(a(H-b)^2 \right)^{p_2} \quad (3)$$

where H is the water level (m). Rainfall spatial variability has not been considered in SF models thus far. Therefore, an attempt has been made to address this issue by introducing a new parameter, γ in the continuity equation of GSF model as follows:

$$\frac{ds}{dt} = \gamma R + I - E - O - Q - q_l \quad (4)$$

The groundwater-related loss was defined by considering the concept of the soil moisture parameter tank (SMPT) model (Ando et al. 1982) and is given as,

$$q_l = \left\{ \begin{array}{ll} k_3(s-z) & (s \geq z) \\ 0 & (s < z) \end{array} \right\} \quad (5)$$

where k_3 and z are the parameters. The storage (s) in the watersheds should be larger than the infiltration hole height (z) to be contributed to groundwater recharge, as shown in Online Resource 1. Substituting Eq. (3) into Eq. (4) results in a second-order ordinary differential equation (ODE) as follows:

$$k_2 \frac{d^2}{dt^2} (a(H-b)^2)^{p_2} = -k_1 \frac{d}{dt} (a(H-b)^2)^{p_1} + \gamma R + I - E - O - a(H-b)^2 - q_l \quad (6)$$

By numerically solving this second-order ODE, the water level (H) can be estimated. The proposed GSF model is a 9-parameter model with parameters k_1 , k_2 , k_3 , p_1 , p_2 , z , γ , a , and b . Other models considered in this study are (i) 8-parameter model – GSF model without parameter γ , (ii) 7-parameter model – GSF model with fixed values of parameters a and b obtained from an established rating curve, and (iii) 6-parameter model – GSF model without parameter γ and with fixed values of parameters a and b .

2.2 Model Calibration and Validation

The shuffled complex evolution-University of Arizona (SCE-UA) method proposed by Duan et al. (1992) was used to estimate the optimal parameter values for the GSF model with root mean square error (RMSE) as the objective function. The search range of parameters was carefully determined as shown in Table 1 by reviewing the literature of previous studies (Padiyedath et al. 2018a; Prasad 1967; Sugiyama et al. 1997; Takasaki et al. 2009) except for parameters γ , a , and b . For parameter γ , the maximum possible value was set to 10 in this study to incorporate the effect of a ten-times higher magnitude rainfall near the basin outlet compared to the low basin-average rainfall. Finally, the search range of parameters a and b was set based on their values obtained from an established rating curve. The calibration was conducted using two data scenarios: (i) an individual event-based scenario where individual flood events were used and (ii) an all event-based scenario where all the available events were used for the model calibration which was further used to validate the model.

The model performances were assessed using RMSE, Nash-Sutcliffe efficiency (NSE) (Nash and Sutcliffe 1970), and other error functions of percentage error in peak water level (PEP), percentage error in area under the water level hydrograph (PEA) (Padiyedath et al. 2018a). Furthermore, the Akaike Information Criterion (AIC), and Akaike weight (AW) were also used to identify the most effective model based on the number of optimized parameters. The corrected AIC (AIC_C) score was used to correct for small data samples (Hurvich and Tsai 1989). The most effective model is that with the lowest AIC_C score (Akaike 1981; Akaike 1998) and highest AW (Hurvich and Tsai 1989).

Table 1 Description and search range of GSF model parameters

Parameter	Definition	Detailed description	Search range
k_1	Physical watershed characteristics (Sugiyama et al. 1997)	Basin area, Stream length	[0, 500]
k_2	Loop relationship between the storage and discharge (Prasad 1967)	Channel characteristics, Basin shape	[0, 5000]
k_3	Groundwater related loss	Rate factor of groundwater recharge	[0, 1]
p_1	Index of flow regime (Sugiyama et al. 1997)	Flow pattern based on various land use conditions	[0, 1]
p_2	Non-linear unsteady flow effects (Hoshi and Yamaoka 1982)	Factor decides the rate of change of discharge	[0, 1]
z	Infiltration hole height	Minimum water storage required to be contributed to groundwater	[0, 500]
γ	Rainfall factor	Correction coefficient of uncertain rainfall resulted from its spatial variability in the basin	[0, 10]
a	Rating curve constant	Constant that represents the station characteristics	[0, 100]
b	Rating curve constant	Constant that represents the gauge reading corresponding to zero discharge	[-100, 100]

2.3 Sensitivity Analysis

Sensitivity analysis (SA) is used to examine how a model output is influenced by the uncertainty in the model parameters and inputs (Neumann 2012). SA methods can be classified as either local or global (Đukić and Radić 2016; Liu et al. 2016). In this study, we utilized the Morris global sensitivity analysis (Morris 1991) which is a screening method based on elementary effects to identify a subset of the parameter that has the greatest influence on the output.

Consider a model for which an output y is a function of k parameters θ_i , $i = 1, 2, \dots, k$. For a given value of θ , the elementary effect of the i^{th} parameter is given by the following equation:

$$d_i(\theta) = \frac{f(\theta_1, \theta_2, \dots, \theta_{i-1}, \theta_i + \Delta, \theta_{i+1}, \dots, \theta_k) - f(\theta)}{\Delta} \quad (7)$$

where Δ is the magnitude of step, which is a multiple of $1/(p-1)$; p is the number of levels over which the variables can be sampled; and $f(\theta)$ is the target function value for the parameter vector θ (Shin et al. 2013). Each θ_i will be assumed to be scaled to take on values within the interval [0, 1] and scaled to appropriate ranges of the input variables after performing the analysis to compute the elementary effect (Morris 1991). Campolongo et al. (2007) suggested a convenient choice for the Morris parameters that the p is preferentially even ($p = 10$ in this study) and Δ is equal to $p/2(p-1)$. The d_i calculation process has repeated several times (r),

and the mean (μ) and standard deviation (σ) values of the r samples of d_j have used as Morris sensitivity indices. Instead of using μ , Campolongo et al. (2007) used an improved measure $\mu_i^* = \frac{1}{r} \sum_{j=1}^r |d_j(\theta_i)|$, which is the mean of the absolute values of the r samples of the elementary effect of the i^{th} parameter. Therefore, this study used μ^* with $r=20$ because the r value is typically between 10 and 50, as explained by Campolongo et al. (2007). A high μ^* value implies that the high sensitivity of parameter on the target function and a high σ value indicates that the parameter has strong interactions with other parameters (Morris 1991; Shin et al. 2013; van Griensven et al. 2006).

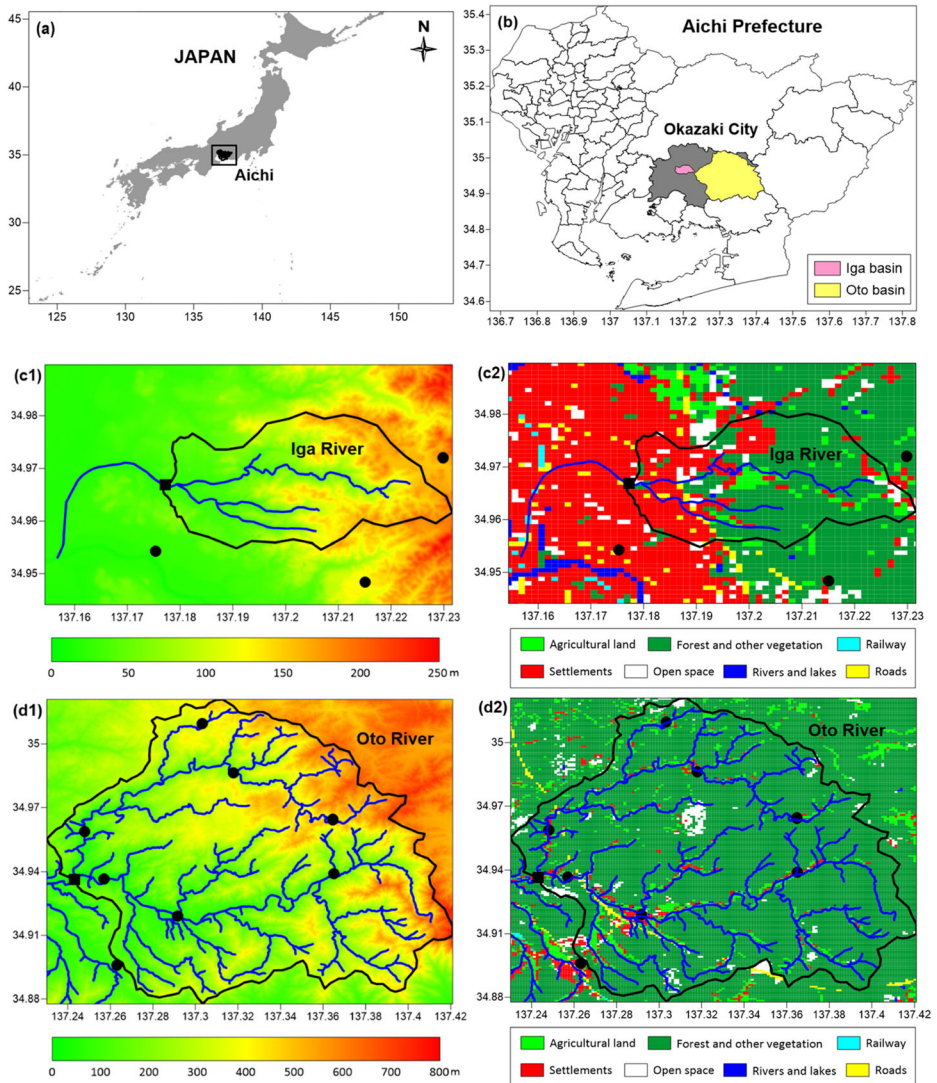


Fig. 1 Index map of (a) Japan, (b) Iga basin and Oto basin within the Okazaki city of Aichi prefecture, (c1) Topographic map of Iga basin, (c2) Land use map of Iga basin, (d1) Topographic map of Oto basin, and (d2) Land use map of Oto basin. The solid rectangle and circle are the water level and rain gauge stations respectively

3 Study Area and Data Used

The proposed GSF model was applied in the two watersheds of Iga and Oto within Okazaki City, Aichi Prefecture, Japan (Fig. 1). Okazaki City is the third-largest city in Aichi Prefecture with a humid subtropical climate and an elevation ranging from 0 to 789 m above sea level (Rimba et al. 2017). The central city consists of alluvial plains, whereas the eastern part of the city is mountainous area; the remainder is lowland area which has an altitude ranging from 0 to 300 m (Okazakishi 2019). Precipitation occurs throughout the year with an annual rainfall of approximately 1500 mm.

Iga River (small to medium-sized semi-urban watershed with an area of approximately 9.6 km² at Iga Bridge) is a narrow river with low channel capacity and flat riverbed. The design discharge capacity of the Iga basin is 154 mm/day for a 5-year return period. The basin mainly consists of red-yellow soil, other soil (impervious surfaces, rock, etc.), and low land soil. The drainage density, urbanization rate, and slope of the Iga basin are around 0.42 km⁻¹, 40%, and 10.7° respectively. The Oto basin (large rural watershed with an area of approximately 216.46 km² at Chiharazawa) originates from the Mt. Tomoe in the eastern parts of the Okazaki City and flows further towards west. For a return period of 20 years, the design discharge capacity is 352 mm/day. The basin has a low drainage density of 0.13 km⁻¹ compared with the Iga basin. The urbanization rate and the slope of the basin are around 3.3% and 19.5° respectively. The major soil type of the basin is brown forest soil, followed by the red-yellow soil and the immature soil. Both the Iga and Oto rivers are the tributaries of the Yahagi River, a first-class river in Japan. During the past several decades, heavy rains and flooding have occurred in the basins as a result of typhoons and intensive localized rainfall in which the flood in 2008 was the most severe with a rainfall intensity of approximately 146.5 mm/h (Okazakishi 2015). Approximately 620 houses were flooded above floor levels

Table 2 Characteristics of the selected events for Iga and Oto basins

Event no.	Event date	Peak H (m)	R ₆₀ (mm)	Average R (mm)	Meteorological factors
Calibration events – Iga basin (2013–2015)					
1	10/9/2015	24.1	32.9	40.3	Typhoon
2	7~8/9/2013	23.9	42.9	44.8	Frontal event
3	8~9/9/2015	23.9	18.6	134.2	Typhoon
4	15~16/10/2013	23.7	14.3	138.7	Typhoon
5	26~27/5/2014	23.7	14.2	68.9	Frontal event
Validation events – Iga basin (2016)					
1	19~21/9/2016	24.5	47.9	161.5	Typhoon
2	18~19/3/2016	23.6	17.7	51.0	Frontal event
Calibration events – Oto basin (2013–2015)					
1	15~16/9/2013	5.7	56.1	229.1	Typhoon
2	8~9/9/2015	2.6	14.3	119.5	Typhoon
3	24~25/9/2014	2.5	22.1	106.3	Typhoon
4	29~30/3/2014	2.5	20.3	108.5	Frontal event
5	16~18/8/2015	2.4	29.8	77.1	Frontal event
Validation events – Oto basin (2016)					
1	3~4/5/2016	2.0	24.8	81.4	Frontal event
2	22~23/12/2016	1.8	20.9	69	Frontal event

(Adachi 2009). Recently, Typhoon Malakas caused torrential rainfall in 2016 with an intensity greater than 100 mm/h.

The rainfall and water level data at 10-min intervals were collected from the Okazaki City Government during the period 2013–2016 for the study. The basin-average rainfall was determined using the Thiessen polygon method from the rain gauges scattered over the basin. Five target events were selected from the data for the calibration and two events that are not included in the model calibration were chosen for model validation (Table 2). The inflow component (I), water intake (O), and evapotranspiration (E) were set at 0 as there is no intake to and from the target basins and the evapotranspiration during heavy rainfall is insignificant.

4 Results and Discussion

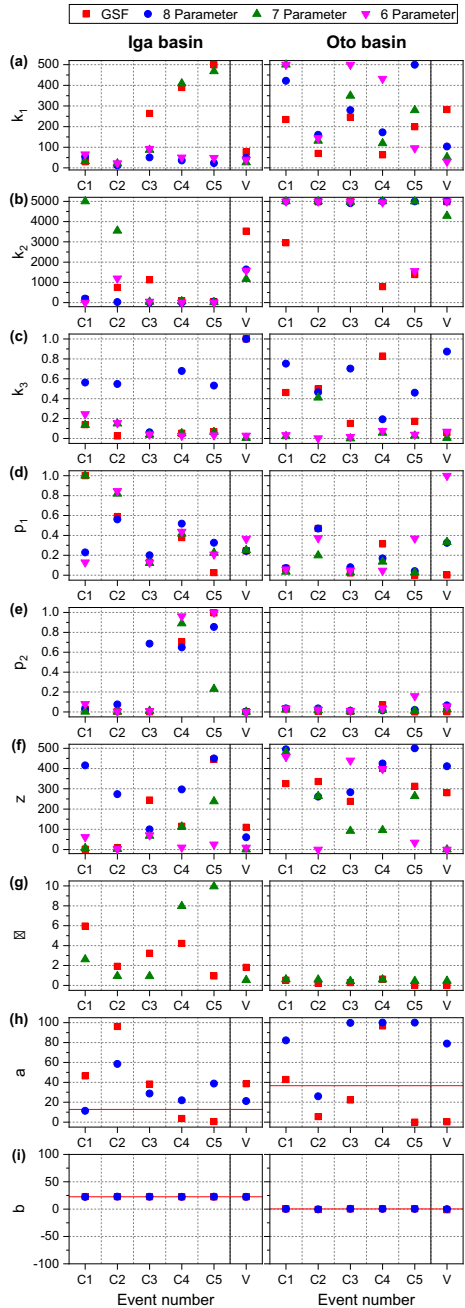
4.1 Model Calibration

Figure 2a–f shows the calibrated parameters k_1 , k_2 , k_3 , p_1 , p_2 , and z , respectively. These are associated with all the four considered models. The large Oto basin exhibited relatively higher k_1 values compared with Iga basin which further confirms the results of Park et al. (2012). According to them, the parameter k_1 has high relevance to the basin characteristics in such a manner that any increase in the basin area, as well as the stream length, will lead to an increase in parameter k_1 . The parameter k_2 was found to depend on the main channel characteristics, basin shape, and rainfall amount and duration, among others (Prasad 1967) which resulted in higher k_2 values for the Oto basin. The GSF model showed high variability in parameter k_3 only for the Oto basin, whereas the p_1 values were almost similar for all the models in both basins. The p_2 values of the Iga basin were higher compared to those of the Oto basin, which further indicates a relatively higher unsteady flow in the semi-urban Iga basin (Hoshi and Yamaoka 1982). There is high variability in the z values of all the models and the events for both basins.

The GSF and 7-parameter models showed γ values either greater than one or equal to one for the Iga basin (Fig. 2g). This represents a higher rainfall magnitude near the outlet compared to the basin-average rainfall. On the other hand, the Oto basin showed values less than one for all the models which indicate a higher basin-average rainfall compared to the rainfall near the basin outlet. Figure 2h–i demonstrates the rating curve constants a and b , in which the parameter a varies from event to event for both basins and all the models. The calibrated values parameter a are far compared to the fixed value represented by the red line, whereas the parameter b exhibited a high level of agreement with the fixed value in both basins.

Furthermore, to assess the significance of the optimized value of γ in the GSF model, the spatial variability of total rainfall was plotted by interpolating the rainfall received at the gauging stations using the Kriging interpolation technique, which has been widely used for data interpolation (Azhiokodan and Yokoyama 2019). It can be seen from Fig. 3a1–a3 that heavy rainfall occurred near the watershed outlet, which produces an immediate and intensive response at the semi-urban Iga basin outlet. However, the basin-average rainfall of these events (Table 2) is quite low compared to the high rainfall at the outlet. At this point, the GSF model increased the γ values greater than one to incorporate the effect of this actual rainfall near the outlet. In contrast, the Oto basin outlet received a small amount of rainfall compared to the basin-average rainfall, and the high rainfall occurred at a specific location farther from the outlet point which will generate a delayed and diminished response as shown in Fig. 3b1–b3.

Fig. 2 The calibrated parameters of GSF, 8-, 7-, and 6-parameter models for the Oto and Iga basins. ‘C’ indicates calibrated parameters from individual events and ‘V’ indicates the calibrated parameters from all the events. The red line in (h) and (i) represents the fixed values of parameters a and b obtained from the established rating curve



The use of basin-average rainfall may lead to the overestimation of water level, and a reduced γ value is needed to compensate for this effect which further resulted in a γ value less than one.

It is evident from the results that the same set of model parameters cannot be used for basins with dissimilar physical characteristics (Pickup 1977). Generally, during the parameter

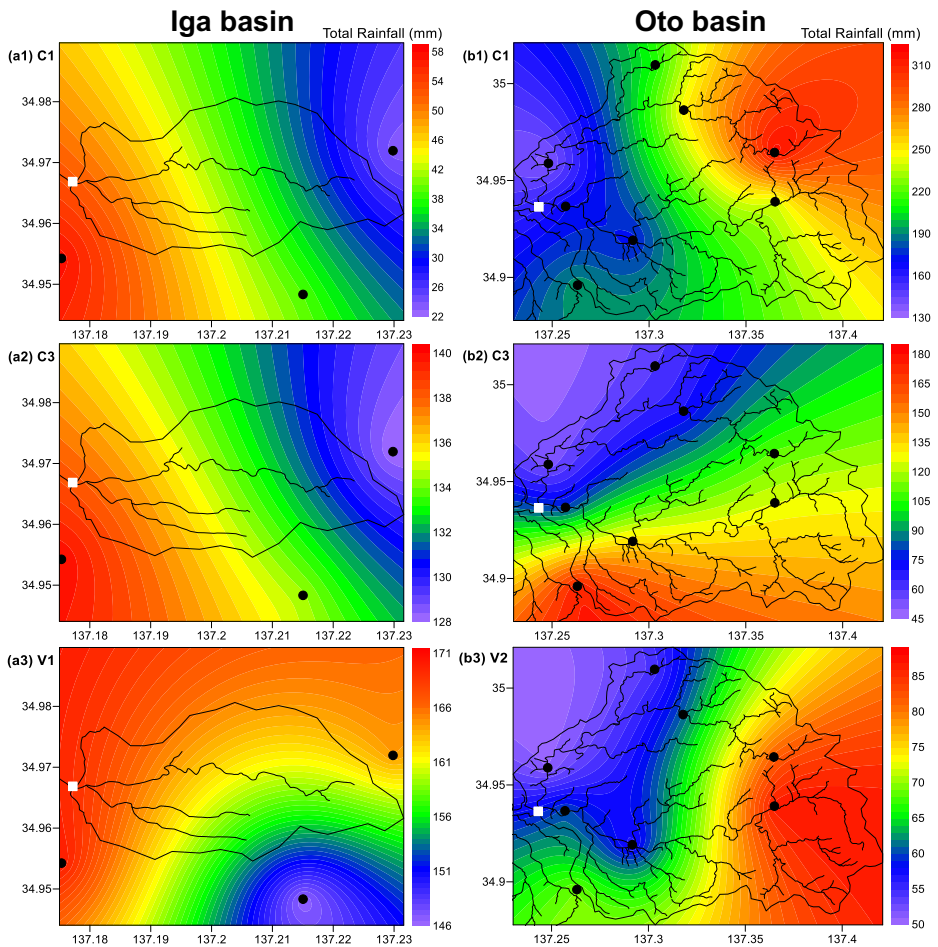


Fig. 3 Spatial distribution of total rainfall during calibration and validation events for Iga basin (**a1–a3**) and Oto basin (**b1–b3**). ‘C’ and ‘V’ indicate the calibration and validation respectively (circle and square represent rain gauge and water level stations respectively)

estimation, the model attempts to optimize the parameters based on its structure to obtain the best combination, which will lead to better performance. However, it is worth mentioning that no calibration can guarantee the uniqueness of the obtained parameter sets because of a concept called equifinality (Beven 1993).

4.2 Hydrograph Reproducibility

It is clear from Fig. 4a1–a3 of the Iga basin that the 9-parameter GSF model nearly overlaps with the observed water level hydrograph and reproduces the shape slightly better than that of the other models. During event 1, the peak estimated by the GSF model was most close to the observed peak compared to the other models. The low hydrograph reproducibility of the 8 and 6-parameter models, particularly during event 1, indicates that the incorporation of γ is indispensable to achieve better performance. Figure 4b1–b3 of the Oto basin shows that the

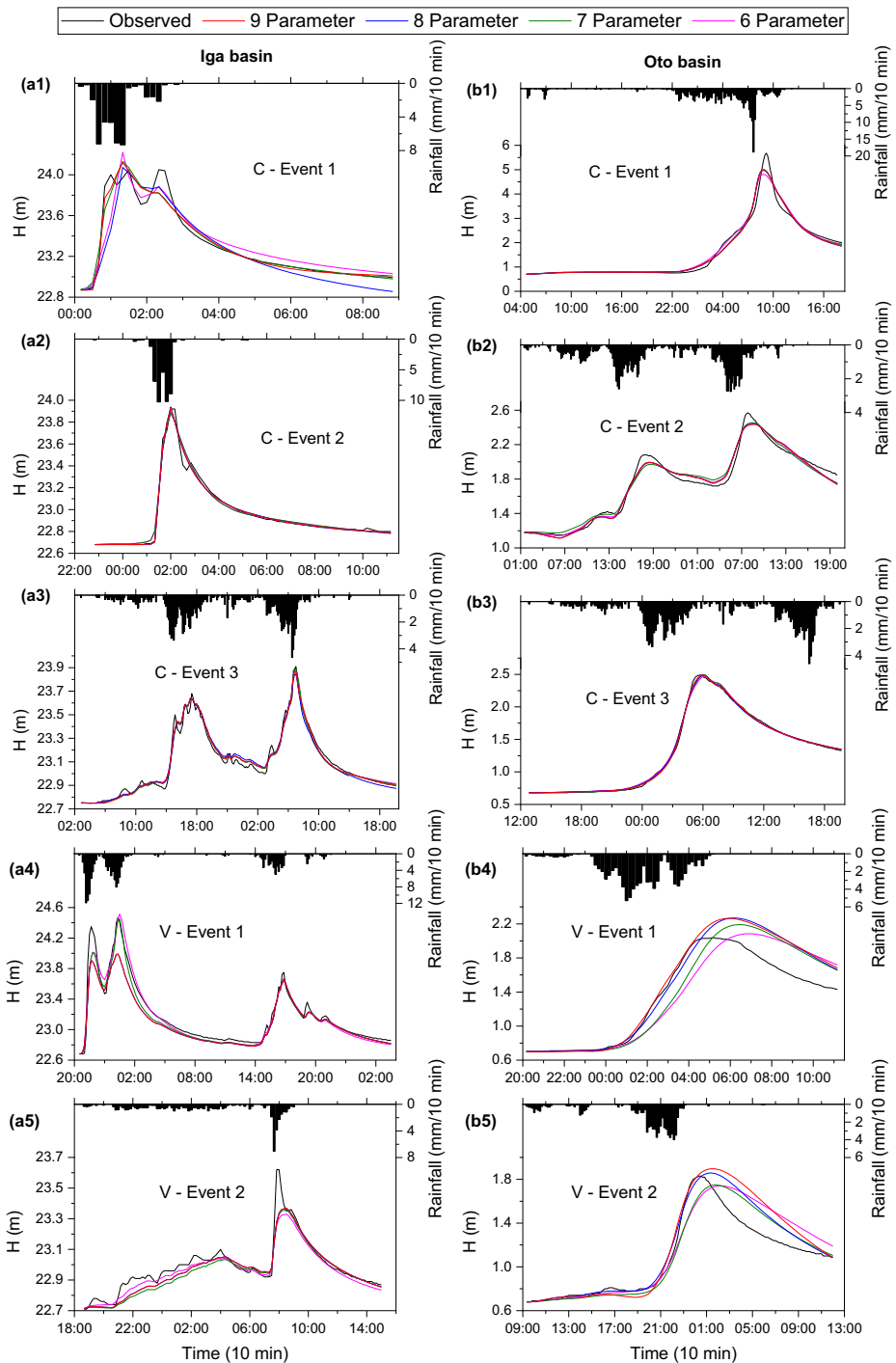


Fig. 4 The reproduced hydrographs by the models for Iga basin (a1-a5) and Oto basin (b1-b5) during calibration and validation ('C' and 'V' indicate the calibration and validation respectively)

GSF model, along with the other models, reproduced the shape of the observed hydrograph with small discrepancies. However, likewise in the Iga basin, the GSF model best simulated the hydrograph as well as peak water level compared to those of other models.

On the other hand, the model validation for the Iga basin illustrated in Fig. 4a4-a5 shows that all the models considerably underestimated the peak water level during both validation events. The inability of the models to predict the peak water level of validation event 1 can be attributed to their low extrapolation potential outside the range of the calibration data set. The GSF model along with other models significantly deviated from the observed hydrograph at the recession limb during the validation in the Oto basin (Fig. 4b4-b5). However, the GSF model accurately reproduced the rising limb compared to other models. The results further

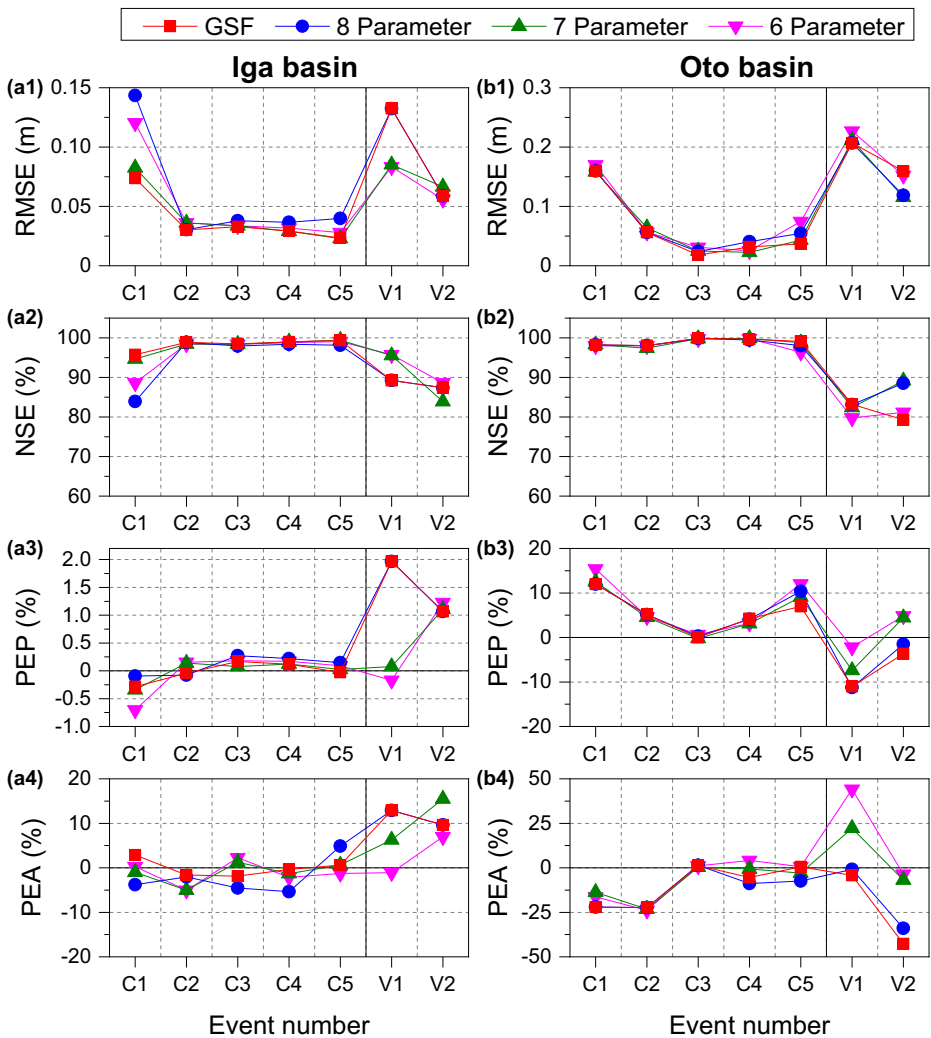


Fig. 5 The performance evaluation of different models during calibration and validation for Iga basin (a1-a4) and Oto basin (b1-b4). ‘C’ and ‘V’ indicate the calibration and validation respectively

revealed that none of the models showed consistent performance during validation in both basins.

Further, the model performance was evaluated using RMSE, NSE, and the other error functions as shown in Fig. 5. Figure 5a1-b1, a2-b2 shows that the GSF model generates the lowest RMSE values and highest NSE values for all the calibration events, whereas the performance was low during the validation events in both the basins. The GSF model was followed by the 7-parameter model, which also considered the effect of parameter γ . Figure 5a3-a4 depict that the PEP and PEA values are close to zero in the Iga basin and not greater than 1% and 10%, respectively, during calibration. On the contrary, the 7 and 6-parameter models demonstrated low PEP and PEA values during validation. In the Oto basin, the PEP and PEA values were within 20% and 50% respectively, as shown in Fig. 5b3, b4. The results also reveal that all the models have a consistent performance during calibration, whereas the performance highly varies during validation.

4.3 AIC Aspect

Figure 6a1-b1 shows the AIC_C values of different models for both basins. It can be seen from Fig. 6a1 that the models showed similar AIC_C values during calibration except for the 8-parameter model. However, during the validation, the 6-parameter model with the least number of parameters exhibited the lowest AIC_C values. During calibration in the Oto basin,

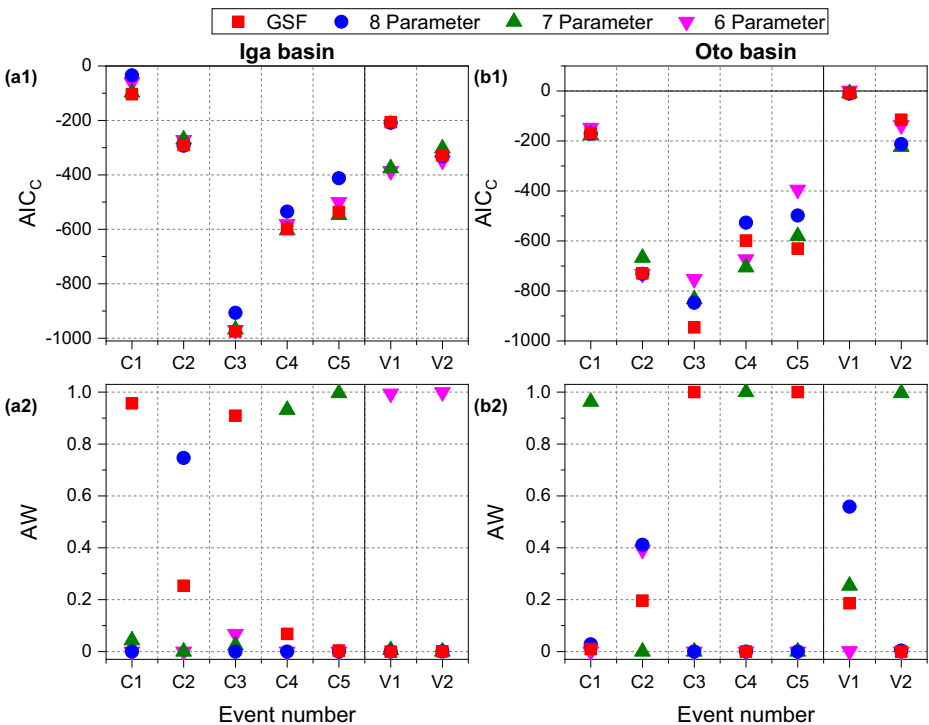


Fig. 6 The summary of Akaike information criterion (AIC) results of corrected AIC (AIC_C) and Akaike weight (AW) values of the models for Iga basin (a1-a2) and Oto basin (b1-b2)

the GSF model showed the lowest AIC_C values in two events (events 3 and 5), and the 7-parameter model had the lowest values during event 4. All the models showed identical AIC_C values in the remaining events during calibration and validation. From Fig. 6a1-b1, it is not easy to clearly distinguish the difference among all the models. Therefore, we analyzed the AIC_C values using AW to depict the differences among the models.

The model with the highest AW is considered to be the best. Figure 6a2-b2 shows that the GSF and 7-parameter models received the highest weights during two calibration events and were greater than 0.8. The 8-parameter model received the highest AW value during event 2 in both basins and was followed by the GSF model. The high AW values of the GSF and 7-parameter models during most of the calibration events for both basins can be ascribed to the effect of the incorporated parameter γ . This further indicates that the parameter γ will act as a water balance corrector. During validation, none of the models exhibited a consistent performance based on the AW values. The AIC analysis revealed that both the GSF and 7-parameter models showed comparable performance, whereas the remaining models without parameter γ showed relatively low performance.

4.4 Sensitivity Analysis of the GSF Model

Figure 7 shows the screening plot from the Morris sensitivity analysis with μ^* values on the x-axis and σ values on the y-axis (Zhan et al. 2013) for the objective function RMSE. It is clear from the figure that the parameter b has the highest μ^* value for both basins. This further indicates that it is the most sensitive parameter of the GSF model because it represents the gauge reading corresponding to zero discharge. Parameter b was followed by parameter p_2 because it constitutes the non-linear unsteady flow effects. Apart from b and p_2 , the ranking order of the sensitive parameters was different in both basins. In the Iga basin, the parameters p_2 , p_1 , b , k_2 and a exhibited higher σ values which show their strong interactions with other parameters, whereas the remaining parameters showed relatively low interaction. In the Oto basin, parameter b showed the strongest interaction with other parameters due to its highest σ value. The parameter p_2 portrayed high interaction with the other parameters after parameter b , and the remaining parameters showed relatively low interaction. The sensitivity analysis showed that the order of sensitive parameters changed between basins. Van Griensven et al. (2006) examined the parameter sensitivity of the Soil and Water Assessment Tool (SWAT)

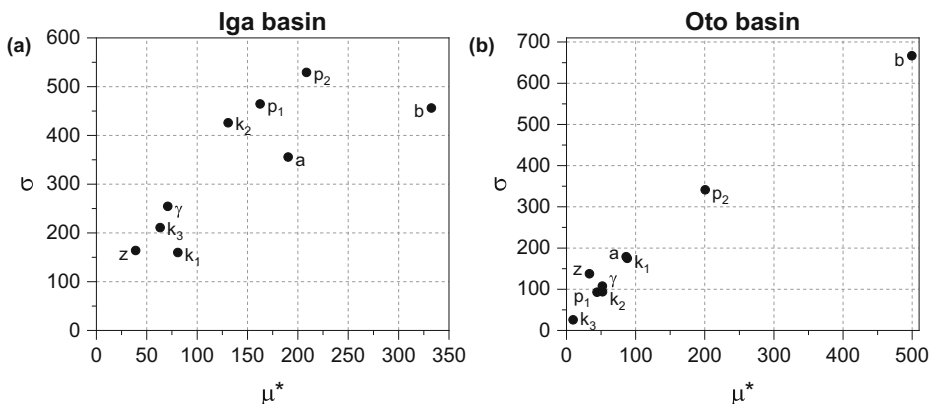


Fig. 7 Morris sensitivity indices for the objective function RMSE in (a) Iga basin and (b) Oto basin

model and found that the sensitive parameters will vary between catchments. Shin et al. (2013) strengthened the results of van Griensven et al. (2006) that the sensitivities of parameters in a rainfall-runoff model are site-specific and cannot be assumed from previous work in other catchments.

Notably, the models with many parameters did not always provide the best predictions, which further shows that complexity alone cannot guarantee good and reliable performances (Perrin et al. 2001). The model parameters are subject to change from event to event, and hence the prediction of future events is a challenging task using the model with fixed calibrated parameters. However, one solution to tackle this issue is the real-time prediction of the model parameters using data assimilation techniques.

5 Conclusions

A generalized storage function (GSF) model was proposed for the water level prediction in which the spatial distribution of rainfall over the basin was considered, and all the possible inflow and outflow components were incorporated (if there is any). The proposed GSF model, along with three other models, was then applied for two watersheds of Japan. The hydrograph reproducibility of different models was analyzed, and the GSF model exhibited higher performance during calibration. None of the models showed consistent performance during validation. In comparison with the GSF model, the 7-parameter model, whose rating curve parameters were obtained from actual basin observations, was expected to provide good results. Based on the AIC aspect, the GSF model outperformed other models during most of the events. Therefore, we can conclude that the GSF model is much more effective using optimized rating curve constants for the use in ungauged and partially gauged watersheds. Any of the considered models, including the GSF model, were not so reliable during validation.

This study proposes an effective water level estimation system which can be used for making sound decisions on a wide variety of water management issues. However, there is a need to improve the model for application in an operational context using data assimilation approaches. The authors focus on these points and will carry out an effort for real-time water level prediction using the proposed GSF model.

Acknowledgements This study was carried out as a part of the research project entitled “Study on guerrilla rainstorm, flood, and water pollution in megacity urban watersheds - Countermeasures against megacity urban water-related disasters bipolarized by climate change” supported by Tokyo Metropolitan Government, Japan (Represented by Prof. Akira Kawamura). Thanks are also given to the Okazaki City Government for providing the dataset.

Compliance with Ethical Standards

Conflict of Interest None.

References

Adachi T (2009) Flood damage mitigation efforts in Japan. In: Proceedings of the fifth US-Japan conference on flood control and water resources management, Tokyo, Japan, 27–29 September 2009

- Akaike H (1981) Likelihood of a model and information criteria. *J Econ* 16:3–14. [https://doi.org/10.1016/0304-4076\(81\)90071-3](https://doi.org/10.1016/0304-4076(81)90071-3)
- Akaike H (1998) Information theory and an extension of the maximum likelihood principle. Springer, New York, pp 199–213. https://doi.org/10.1007/978-1-4612-1694-0_15
- Ando Y, Takahashi Y, Mao H, Jiansi J (1982) A hydrological cycle of hillslope basins and its change by urbanisation. *Proc 26th Japanese conf on hydraulics, JSCE*, pp 251–260
- Andrews FT, Croke BFW, Jakeman AJ (2011) An open software environment for hydrological model assessment and development. *Environ Model Softw* 26:1171–1185. <https://doi.org/10.1016/j.envsoft.2011.04.006>
- Azhikodan G, Yokoyama K (2019) Seasonal Morphodynamic evolution in a Meandering Channel of a macrotidal estuary. *Sci Total Environ* 684:281–295. <https://doi.org/10.1016/j.scitotenv.2019.05.289>
- Baba H, Hoshi K, Hashimoto N (1999) Synthetic storage routing model coupled with loss mechanisms. *Proc Hydraul Eng Japan Soc Civ Eng* 43:1085–1090. <https://doi.org/10.2208/prohe.43.1085>
- Beven K (1993) Prophecy, reality and uncertainty in distributed hydrological modelling. *Adv Water Resour* 16(1):41–51. [https://doi.org/10.1016/0309-1708\(93\)90028-E](https://doi.org/10.1016/0309-1708(93)90028-E)
- Bubeck P, Botzen WJ, Aerts JC (2012) A review of risk perceptions and other factors that influence flood mitigation behavior. *Risk Anal* 32:1481–1495. <https://doi.org/10.1111/j.1539-6924.2011.01783.x>
- Campolongo F, Cariboni J, Saltelli A (2007) An effective screening design for sensitivity analysis of large models. *Environ Model Softw* 22:1509–1518. <https://doi.org/10.1016/j.envsoft.2006.10.004>
- Chen YC, Hsu YC, Kuo KT (2013) Uncertainties in the methods of flood discharge measurement. *Water Resour Manag* 27:153–167. <https://doi.org/10.1007/s11269-012-0174-2>
- Domenghetti A, Castellarin A, Brath A (2012) Assessing rating-curve uncertainty and its effects on hydraulic model calibration. *Hydrol Earth Syst Sci* 16:1191–1202. <https://doi.org/10.5194/hess-16-1191-2012>
- Duan QY, Sorooshian S, Gupta VK (1992) Effective and efficient global optimization for conceptual rainfall-runoff models. *Water Resour Res* 28:1015–1031. <https://doi.org/10.1029/91WR02985>
- Đukić V, Radić Z (2016) Sensitivity analysis of a physically based distributed model. *Water Resour Manag* 30:1669–1684. <https://doi.org/10.1007/s11269-016-1243-8>
- Hoshi K, Yamaoka H (1982) A relationship between kinematic wave and storage routing models. *Proc 26th Japanese Conf on Hydraul JSCE*, pp 273–278. <https://doi.org/10.2208/prohe1975.26.273>
- Hurvich CM, Tsai CL (1989) Regression and time series model selection in small samples. *Biometrika* 76:297–307. <https://doi.org/10.2307/2336663>
- Karbasi M, Shokoohi A, Saghafian B (2018) Loss of life estimation due to flash floods in residential areas using a regional model. *Water Resour Manag* 32:4575–4589. <https://doi.org/10.1007/s11269-018-2071-9>
- Kimura T (1961) The flood runoff analysis method by the storage function model. The Public Works Research Institute, Ministry of Construction
- Liu Y, Chaubey I, Bowling LC, Bralts VF, Engel BA (2016) Sensitivity and uncertainty analysis of the L-THIA-LID 2.1 model. *Water Resour Manag* 30:4927–4949. <https://doi.org/10.1007/s11269-016-1462-z>
- Morris MD (1991) Factorial sampling plans for preliminary computational experiments. *Technometrics* 33:161–174. <https://doi.org/10.1080/00401706.1991.10484804>
- Nash JE, Sutcliffe JV (1970) River flow forecasting through conceptual models part I - a discussion of principles. *J Hydrol* 10:282–290. [https://doi.org/10.1016/0022-1694\(70\)90255-6](https://doi.org/10.1016/0022-1694(70)90255-6)
- Neumann MB (2012) Comparison of sensitivity analysis methods for pollutant degradation modelling: a case study from drinking water treatment. *Sci Total Environ* 433:530–537. <https://doi.org/10.1016/j.scitotenv.2012.06.026>
- Okazakishi (2015) Creating master plan of Okazaki municipal water environment: draft; Master Plan of Okazaki Municipal Water Environment: Okazaki, Japan
- Okazakishi (2019) Current status and problems of biodiversity, environmental policy division. Available online: <http://www.city.okazaki.lg.jp/1300/1303/1326/p011109.html>. Accessed 22 Apr 2019
- Padiyedath SG, Kawamura A, Takasaki T, Amaguchi H, Azhikodan G (2018a) An effective storage function model for an urban watershed in terms of hydrograph reproducibility and Akaike information criterion. *J Hydrol* 563:657–668. <https://doi.org/10.1016/j.jhydrol.2018.06.035>
- Padiyedath SG, Kawamura A, Takasaki T, Amaguchi H, Azhikodan G (2018b) Performance evaluation of urban storage function (USF) model compared with various conventional storage function models for an urban watershed. *J Japan Soc Civ Eng Ser B1 (Hydraul Eng)* 74(4):973–978. https://doi.org/10.2208/jscejhe.74.1_973
- Park M, Kim D, Kwak J, Kim H (2012) Evaluation of parameter characteristics of a storage function model. *J Hydrol Eng* 19:308–318. [https://doi.org/10.1061/\(asce\)he.1943-5584.0000678](https://doi.org/10.1061/(asce)he.1943-5584.0000678)
- Perrin C, Michel C, Andréassian V (2001) Does a large number of parameters enhance model performance? Comparative assessment of common catchment model structures on 429 catchments. *J Hydrol* 242:275–301. [https://doi.org/10.1016/S0022-1694\(00\)00393-0](https://doi.org/10.1016/S0022-1694(00)00393-0)

- Pickup G (1977) Potential and limitations of rainfall-runoff models for prediction on ungauged catchments: a case study from the Papua New Guinea highlands. *J Hydrol N Z* 16(1):87–102
- Prasad R (1967) A nonlinear hydrologic system response model. *J Hydraul Div ASCE* 93-HY4:201–221
- Rimba A, Setiawati M, Sambah A, Miura F (2017) Physical flood vulnerability mapping applying geospatial techniques in Okazaki City, Aichi prefecture, Japan. *Urban Sci* 1(1):7. <https://doi.org/10.3390/urbansci1010007>
- Sahoo B, Saritha PG (2015) Estimating Floods from an ungauged river basin using GIUH-based Nash model. ISFRAM 2014. Springer, Singapore. https://doi.org/10.1007/978-981-287-365-1_11
- Seckin N, Guven A (2012) Estimation of peak flood discharges at ungauged sites across Turkey. *Water Resour Manag* 26:2569–2581. <https://doi.org/10.1007/s11269-012-0033-1>
- Shin MJ, Guillaume JHA, Croke BFW, Jakeman AJ (2013) Addressing ten questions about conceptual rainfall-runoff models with global sensitivity analyses in R. *J Hydrol* 503:135–152. <https://doi.org/10.1016/j.jhydrol.2013.08.047>
- Sivapragasam C, Muttil N (2005) Discharge rating curve extension – a new approach. *Water Resour Manag* 19: 505–520. <https://doi.org/10.1007/s11269-005-6811-2>
- Sugiyama H, Kadoya M, Nagai A, Lansley K (1997) Evaluation of the storage function model parameter characteristics. *J Hydrol* 191:332–348. [https://doi.org/10.1016/S0022-1694\(96\)03026-0](https://doi.org/10.1016/S0022-1694(96)03026-0)
- Takasaki T, Tsuchiya T, Masuda N (2005) Prediction of water level in small urban rivers using genetic algorithm approach. *J Japan Soc Civ Eng (Water Engineering Research)* 49:451–456. <https://doi.org/10.2208/prohe.49.451>
- Takasaki T, Kawamura A, Amaguchi H, Araki K (2009) New storage function model considering urban runoff process. *J Japan Soc Civ Eng B* 65(3):217–230. <https://doi.org/10.2208/jscejb.65.217>
- Tamura T, Yamashita A, Muto Y (2013) A method for establishing stage-discharge curve by using rainfall, water level data and runoff model. *J Japan Soc Civ Eng Ser B1 (Hydraul Eng)* 69(4):517–522. https://doi.org/10.2208/jscejhe.69.I_517
- van Griensven A, Meixner T, Grunwald S, Bishop T, Diluzio M, Srinivasan R (2006) A global sensitivity analysis tool for the parameters of multi-variable catchment models. *J Hydrol* 324(1–4):10–23. <https://doi.org/10.1016/j.jhydrol.2005.09.008>
- Vatanchi SM, Maghrebi MF (2019) Uncertainty in rating-curves due to manning roughness coefficient. *Water Resour Manag* 33:5153–5167. <https://doi.org/10.1007/s11269-019-02421-6>
- Vaze J, Post DA, Chiew FHS, Perraud J-M, Teng J, Viney NR (2011) Conceptual rainfall–runoff model performance with different spatial rainfall inputs. *J Hydrometeorol* 12:1100–1112. <https://doi.org/10.1175/2011jhm1340.1>
- Vaze J, Jordan P, Beecham R, Frost A, Summerell G (2012) Guidelines for rainfall-runoff modelling. Australian Government Department of Innovation, Industry, Science and Research
- Zhan CS, Song XM, Xia J, Tong C (2013) An efficient integrated approach for global sensitivity analysis of hydrological model parameters. *Environ Model Softw* 41:39–52. <https://doi.org/10.1016/j.envsoft.2012.10.009>

Publisher’s Note Springer Nature remains neutral with regard to jurisdictional claims in published maps and institutional affiliations.

Affiliations

Saritha Padiyedath Gopalan^{1,2} · Akira Kawamura¹ · Hideo Amaguchi¹ · Gubash Azhikodan¹

¹ Department of Civil and Environmental Eng, Tokyo Metropolitan University, 1-1 Minami Osawa, Hachioji, Tokyo 192-0397, Japan

² Centre for Climate Change Adaptation, National Institute for Environmental Studies, 16-2 Onogawa, Tsukuba, Ibaraki 305-8506, Japan